Journal of Clinical Toxicology
ISSN: 2161-0495

Bouwman et al., J Clin Toxicol 2016, 6:3
DOI: 10.4172/2161-0495.1000299

Research Article Open Access

In Vitro, *In Vivo* Comparison of Cyclosporin A Induced Hepatic Protein Expression Profiles

Freek G Bouwman[1#], Anke Van Summeren[1,2#], Anne Kienhuis[3], Leo van der Ven[3], Ewoud N Speksnijder[4], Jean-Paul Noben[5], Johan Renes[1], Jos C S Kleinjans[2] and Edwin C M Mariman[1*]

[#]Both authors contributed equally to this manuscript

[1]Department of Human Biology, Maastricht University, P.O. box 616, 6200 MD Maastricht, The Netherlands

[2]Department of Toxicogenomics, Maastricht University, P.O. box 616, 6200 MD Maastricht, The Netherlands

[3]Laboratory for Health Protection Research, National Institute of Public Health and the Environment (RIVM), Bilthoven, The Netherlands

[4]Department of Toxicogenetics, Leiden University Medical Center, 2300 RC, Leiden, the Netherlands

[5]Hasselt University, Biomedical Research Institute and Transnational University Limburg, School of Life Sciences, Diepenbeek, Belgium

[*]Corresponding author: Dr. Edwin C. M. Mariman, Department of Human Biology, Maastricht University, P.O. box 616, 6200 MD Maastricht, The Netherlands, Tel +31 (0) 43 38; Fax +31 (0) 43 3670976; E-mail: e.mariman@maastrichtuniversity.nl

Received date: April 7, 2016; **Accepted date:** May 12, 2016; **Published date:** May 19, 2016

Abstract

To reduce the amount of laboratory animals which are used to analyze hepatotoxic properties of chemicals and drugs, the development of alternative *in vitro* models is necessary. Ideally these *in vitro* models reflect the *in vivo* toxicological response and cholestasis. In this study the protein expression in livers from C57BL/6 mice after cyclosporin A-induced cholestasis was analyzed. After 25 days of a daily cyclosporine A treatment the cholestatic phenotype was established. An *in vitro* to this *in vivo* study comparison was made by using the results of our previous studies with HepG2 and primary mouse hepatocytes. The *in vivo* proteomics data show cyclosporin A-induced oxidative stress and mitochondrial dysfunction was actually induced, leading to a decreased mitochondrial ATP production and an altered urea cycle. These processes were also altered by cyclosporin A in the *in vitro* models HepG2 and primary mouse hepatocytes. In addition, detoxification enzymes like methyl- and glutathione-S-transferases were differentially expressed after cyclosporin A treatment. Changes in these detoxification enzymes were mainly detected *in vivo*, though primary mouse hepatocytes show a differential expression of some of these enzymes. By means of a functional classification of differentially expressed proteins we demonstrated similarities and differences between *in vitro* and *in vivo* models in the proteome response of cyclosporin A-induced hepatotoxicity.

Keywords: Proteomics; Hepatotoxicity; Cyclosporin A; Liver; *In vivo*

Abbreviations

2DE: 2-Dimensional Gel Electrophoresis; ABC- Transporters: ATP Binding Cassette Transporters; CHOL: Cholesterol; CsA: Cyclosporin A; DIGE: Difference Gel Electrophoresis; GSTs: Glutathione S-Transferases; MALDI-TOF/TOF-MS: Matrix Assisted Laser Desorption Ionization Time-of-Flight Tandem Mass Spectrometry; LC-MSMS: Nano Liquid Chromatography Tandem Mass Spectrometry; TBIL: Total Bilirubin; TBA: Total Bile Acids

Introduction

Novel drugs should be recognized as safe for human exposure. With respect to drug-induced toxicity, hepatotoxicity is prominent, because most drugs are metabolized to be eliminated by the liver. The hepatotoxic properties of chemicals and drugs are usually analyzed in *in vivo* repeated-dose toxicity tests, which involve a high number of laboratory animals. To reduce the amount of laboratory animals, alternative *in vitro* models are currently developed and their screening properties evaluated [1-3]. Ideally these *in vitro* models reflect the *in vivo* toxicological response. Accordingly, *in vitro* to *in vivo* comparisons are necessary. By applying Omics technologies it is possible to measure similar endpoints of drug-induced changes between *in vitro* and *in vivo* which enable a global comparison of both models [4].

Conventional hepatotoxicity assays rely on the analysis of clinical, hematological, and histopathological parameters. While the conventional assays generally measure only a limited set of biological endpoints, Omics technologies offers the possibility to measure multiple endpoints simultaneously in a single experiment. Currently, transcriptomics studies, where thousands of genes are measured simultaneously, have shown to be successful for this purpose [4-6]. However, transcriptomics investigates the relative mRNA levels of genes which often only moderately correlate with the relative abundance of their protein product. This moderate correlation is due to turnover differences of proteins and mRNA [7].

In addition, post-translational modifications and protein interactions are not detected by transcriptomics, which emphasizes the relevance of proteomics. For example, by applying difference gel electrophoresis (DIGE), proteins are separated based on their pI and molecular weight, so different protein isoforms can be visualized [8].

Previously we investigated the proteome of HepG2 cells and primary mouse hepatocytes after exposure to three well-defined hepatotoxicants [9,10]. These were acetaminophen, amiodarone and cyclosporin A (CsA), of which CsA generated the most prominent

response. CsA is an immunosuppressive drug; however, as an adverse side effect it induces cholestasis caused by the inhibition of the bile salt transporters in hepatocytes [11].

The aim of the present study is to identify cholestatic-specific mechanisms *in vivo*, with use of proteomics. Furthermore, we want to compare these results with our previous *in vitro* studies with HepG2 and primary mouse hepatocytes [9,10].

For this purpose the hepatic protein expression from C57BL/6 mice after CsA-induced cholestasis was examined. The development of cholestasis at the proteome level was analyzed after 4, 11 and 25 days of a daily dose of CsA. The cholestatic phenotype was established after 25 days and was confirmed by serum biochemistry and histopathology.

DIGE was used to analyze the differentially expressed proteins induced by CsA. The results from our previous studies with HepG2 [9] and primary mouse hepatocytes [10] were used to establish an *in vitro-in vivo* comparison of CsA-induced protein expression profiles.

Materials and Methods

Chemicals

CsA, CAS-no 59865-13-3, purity minimum 98%, was kindly provided by Novartis, Basel, Switzerland. N,N-dimethylformamide (anhydrous, 99.8%) was purchased from Sigma-Aldrich (Zwijndrecht, The Netherlands), the Protein Assay Kit was from Bio-Rad (Veenendaal, The Netherlands). All chemicals used for DIGE were purchased from GE Healthcare (Diegem, Belgium).

Animals

Male C57BL/6 mice, aged 10 weeks at the start of the treatment period (21-27 g), were obtained from Charles River GmbH, Sulzfeld, Germany. Animals were kept under controlled specific pathogen-free conditions (23°C, 40%-50% humidity) under a 12hour light-dark cycle, and housed in groups of five.

Food and tap water were available ad libitum during the whole experiment. Experiments were conducted at the animal facility of the Leiden University Medical Center, under ethical review in accordance with the Dutch law (DEC 09157).

Animal treatment

For the 25 day repeated dose study, forty animals were assigned to eight groups of five mice per group. For the 4 and 11 day repeated-dose study, twenty-four animals were assigned to six groups of four mice per group. After an acclimatization period, treatment protocols were used in which mice were dosed with CsA in olive oil or with the vehicle only, by oral gavage in a volume of 4 ml/kg body weight, for five times per week (working days) between 2:00 and 4:00 pm. In the 25 day study, mice were treated with CsA up to 80 mg/kg body weight.

This study was used for dose range finding, selecting the dose of 26.6 mg/kg body weight which was determined to be the critical effect dose that induced cholestatic clinical chemistry parameters at 25 days of exposure. The animals were sacrificed by inhalation of CO_2 and heart puncture at four, eleven and twenty-five days post CsA administration. Blood was collected in 0.8 ml Minicollect serum collection tubes (Greiner Bio-One, Alphen aan de Rijn, The Netherlands) for serum chemistry analyses.

The liver samples were frozen in liquid nitrogen and stored at -80°C until the protein isolation. Liver samples of animals treated with 26.6 mg/kg body weight in the 25 day dose range finding study and liver samples of the 4 and 11 day study were used for proteome analysis.

Serum biochemistry

Alanine transaminase (ALT), Aspartate transaminase (AST), Cholesterol (CHOL), total bilirubin (TBIL) and total bile acids (TBA) were analyzed on a Beckman Coulter LX20 Clinical Chemistry Analyzer using Beckman reagent kits (Beckman Coulter B.V., Woerden, The Netherlands) for TBIL, and CHOL, and a Dialab reagent kit (DIALAB GmbH, Neudorf, Austria) for TBA. A student's-T test was performed on the results to determine significant differences.

Histopathology

After 24 hours fixation in 4% neutral buffered formalin, liver samples were stored in 70% ethanol until further processing, which included automated dehydration, embedding in paraffin, sectioning at 5 µm, and staining with hematoxylin and eosin.

Sample preparation

Liver samples were ground into fine powder in liquid nitrogen and homogenized in DIGE labeling buffer containing 7 M urea, 2 M thiourea, 4% (w/v) CHAPS and 30 mM TrisHCl. This mixture was mixed thoroughly and subjected to three cycles of freeze thawing with liquid nitrogen to lyse the cells. The homogenate was vortexed for 1 minute and centrifuged at 20 000g for 30 min at 10°C. The supernatant was collected and stored at -80°C until further analysis. Protein concentrations were determined with the Protein Assay Kit from Bio-Rad (Veenendaal, The Netherlands).

DIGE

The protein labeling and the DIGE were performed as described before [9]. A one-way ANOVA test ($P \leq 0.05$) was used to select the significant differential spots between the experimental groups. In addition, two way ANOVA-treatment, two-way ANOVA-time, and two-way ANOVA-interaction were computed to assign statistically significant changes in spot intensity due to the treatment alone, time alone and due to both treatment and time.

The differentially expressed proteins were excised and identified by matrix assisted laser desorption ionization time of flight tandem mass spectrometry (MALDI-TOF/TOF-MS) according to Bouwman et al. [12]. Protein spots that could not be identified by MALDI-TOF/TOF-MS were further analyzed by nano liquid chromatography tandem mass spectrometry (LC-MSMS) on an LCQ Classic (ThermoFinnigan) as described before [13].

Functional Classification

The proteins differentially expressed after exposure to CsA in HepG2 and primary mouse hepatocytes, were retrieved from previous studies [9,10]. The Panther classification system (http://www.pantherdb.org) was used to compare the effect of CsA upon the protein expression in HepG2, primary mouse hepatocytes and *in vivo* mouse liver. From each experiment the differentially expressed proteins were uploaded onto the Panther classification system.

Furthermore, the Functional Classification Tool of the DAVID Bioinformatics resource 6.7 (http://david.abcc.ncifcrf.gov/) was used to cluster functionally related proteins. For this purpose the differentially expressed proteins from the three experiments were uploaded and classified with the lowest stringency. Afterwards it was retrieved in which experiment these proteins were differentially expressed.

Results

Traditional toxicology parameters

To induce cholestasis C57BL/6 mice were treated with 26.6 mg/kg CsA. Histopathology showed submembraneous vacuolization suggesting cholestasis at 25 days (Figure 1). The plotted serum values per animal for CHOL, TBIL, TBA, ALT and AST are presented in Figure 2.

A change (P<0.1) was observed as early as 4 days treatment up till 25 days for the cholestatic parameters CHOL, TBIL, TBA. The general hepatotoxicity markers ALT and AST did not show a significant increase, indicating that a severe stage with liver damage was not yet reached.

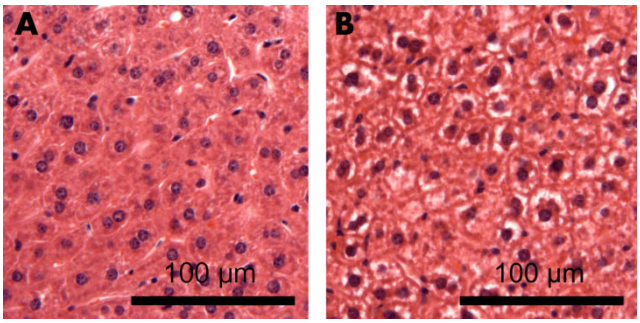

Figure 1: (A) Mouse liver treated with vehicle for 25 days. (B) Submembraneous vacuolization suggestive of cholestasis in mouse liver upon treatment with 26.6 mg/kg body weight for 25 days. Magnification: 60X.

DIGE analysis

To analyze the *in vivo* hepatotoxic effects of CsA, C57BL/6 mice were exposed to CsA for 4, 11 and 25 days with olive oil as a vehicle control. On these time-points the animals were sacrificed and the liver was isolated. The proteins were extracted from these liver samples and the differentially expressed proteins were determined using DIGE. In total 3235 spots could be matched within all images.

With a one-way ANOVA 60 spots were found significantly different ($P \leq 0.05$) between all groups. With a two-way ANOVA analysis 92 spots were significantly different ($P \leq 0.05$) in response to treatment, 12 spots were significantly different ($P \leq 0.05$) in time and 8 spots were differentially expressed for the interaction of the treatment and time ($P \leq 0.05$).

Protein identification

The differential spots were included in a pick list. For spot picking and identification a preparative gel was loaded with 150 µg of the internal standard labeled with 300 pmol Cy2 and run in the same way as the analytical gels. Afterwards, with use of the DeCyder™ 7.0 software (GE Healthcare) the preparative gel was matched with the analytical gels.

Protein identification was performed by in-gel digestion followed by MALDI-TOF/TOF-MS and/or LC-MS/MS analysis. The 96 selected protein spots were identified belonging to 86 different proteins. A total of 19 protein spots were isoforms from 9 proteins due to post-translational modifications or processing of the protein. Figure 3 shows the 2-DE map made from the master gel with the identified differential spots indicated with a number which corresponds to the numbers presented in Table 1.

For the identified protein spots a Tukey's multiple comparison test was performed, from which 4 spots (methylcrotonoyl-CoA carboxylase alpha chain, aconitate hydratase, and two isoforms of carbamoyl-phosphate synthase I) were significantly differential after 4 days treatment of CsA. After 11 days of treatment 8 spots were differentially expressed (alpha enolase, selenium-binding protein 2, NADP-dependent malic enzyme, transketolase, eukaryotic peptide chain release factor subunit 1, pyruvate kinase, superoxide dismutase 2, and indolethylamine N-methyltransferase).

Twenty five days of treatment induced the differential expression of 6 spots (glutathione S-transferase Mu 2, farnesyl pyrophosphate synthetase, selenium-binding protein 2, sulfite oxidase, thiopurine S-methyltransferase and protein disulfide-isomerase).

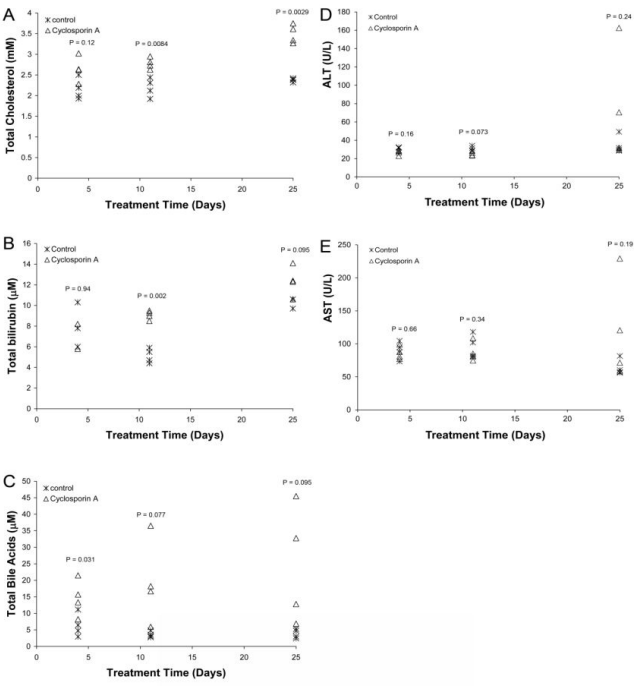

Figure 2: Plotted serum values per animal for (A) Cholesterol, (B) Total Bilirubine, (C) Total Bile Acids, (D) ALT and (E) AST at 4, 11, and 25 days of exposure to 26.6 mg/kg body weight CsA.

In Table 1 the spots are listed with their protein identification and their fold changes between the control and compound. The significant changes are marked with $^{**}P \leq 0.05$ or $^{*}P \leq 0.1$ accordingly Tukey's multiple comparison test.

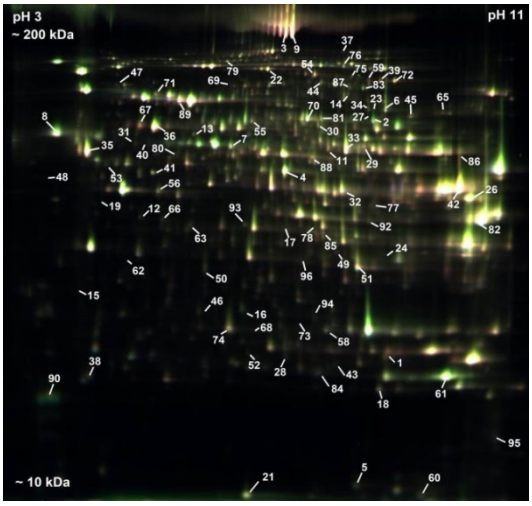

Figure 3: Proteome map of the differentially expressed proteins. The identified spots are indicated with a number which corresponds to the numbers used in Table 1.

Functional classification

Data from HepG2 and primary mouse hepatocytes, were retrieved from previous studies [9,10]. The Venn diagram in Figure 4 illustrates the overlap of differentially expressed proteins induced by CsA in *in vivo* mouse liver, primary mouse hepatocytes and HepG2 cells.

In order to compare the protein expression results in mouse and human cells, only mouse orthologues were used. The overlap of the differentially expressed proteins is the highest between the *in vitro* models PMH and HepG2.

However the *in vivo-in vitro* comparison of CsA-induced hepatotoxicity based on single protein expression shows only a small overlap in the differentially expressed proteins from the different models.

For that reason we made use of the Panther classification system to identify the functional properties of the identified proteins. The differentially expressed proteins in the liver from exposed mice were mostly involved in metabolic process, immune system process and generation of precursor metabolites and energy (Figure 5).

For HepG2 cells and primary mouse hepatocytes the majority of the differential proteins are involved in transport, metabolic and cellular processes (Figure 5). Similar processes between the analyzed *in vitro* systems are cell cycle, cellular processes, developmental processes and cell adhesion (Figure 5).

In all three models CsA altered proteins which belong to transport and a response to stimulus (Figure 5). The Functional Classification Tool of the DAVID Bioinformatics resource 6.7, revealed 12 clusters which are presented in Table 2.

No	Uniprot	Gene name	Protein description	P value				Fold change[5]		
				one-way anova[1]	two-way anova, treatment[2]	two-way anova, time[3]	interaction treatment/ time[4]	CsA4/C4	CsA11/C11	CsA25/C25
Tricarboxylic acid cycle										
39	Q99KI0	Aco2	Aconitate hydratase. mitochondrial precursor	0.018	0.0097	0.11	0.11	-1.17**	-1.01	-1.07
59	Q99KI0	Aco2	Aconitate hydratase. mitochondrial precursor	0.13	0.02	0.93	0.23	-1.13	-1	-1.11
72	Q99KI0	Aco2	Aconitate hydratase. mitochondrial precursor	0.021	0.03	0.036	0.17	-1.14	1	-1.07
32	O88844	Idh1	Isocitrate dehydrogenase [NADP] cytoplasmic	0.038	0.0068	0.4	0.18	1.01	1.11	1.14
56	Q9Z2I9	Sucla2	Succinyl-CoA ligase [ADP-forming] subunit beta. mitochondrial	0.068	0.015	0.11	0.89	-1.09	-1.06	-1.09
69	P16332	Mut	Methylmalonyl-Coenzyme A mutase	0.01	0.028	0.2	0.29	-1.04	-1.14	-1.33
Carbohydrate metabolism										
49	P13707	Gpd1	Glycerol-3-phosphate dehydrogenase [NAD +]. cytoplasmic	0.062	0.014	0.093	0.9	1.1	1.09	1.13
82	Q91Y97	Aldob	Fructose-bisphosphate aldolase B	0.087	0.042	0.6	0.083	-1.05	1.16	1.13

4	P17182	Eno1	Alpha enolase	0.0024	0.00028	0.47	0.052	1.02	1.11**	1.05
25	Q9QXD6	Fbp1	Fructose-1.6-bisphosphatase	0.001	0.0047	0.0009	0.4	1.04	1.1*	1.04
58	Q9DBJ1.	Pgam1	Phosphoglycerate mutase 1	0.0075	0.018	0.0047	0.54	1.07	1.02	1.06
30	P53657	Pklr	Pyruvate kinase. isozymes R/L	0.036	0.0058	0.046	0.17	1.07	1.24**	1.07
85	Q93092	Taldo1	Transaldolase	0.038	0.045	0.18	0.061	-1.04	1.1	1.13
50	P97328	Khk	Ketohexokinase	0.073	0.014	0.75	0.15	-1.01	1.15	1.14
93	Q9DBB8	Dhdh	Trans-1.2-dihydrobenzene-1.2-diol dehydrogenase	0.037	0.22	0.038	0.085	-1.05	1.09	1.07
88	Q9JLJ2	Aldh9a1	4-trimethylaminobutyraldehyde dehydrogenase	0.19	0.05	0.87	0.18	-1.02	1.12	1.09
Urea cycle										
17	Q61176	Arg1	Arginase-1	0.0069	0.0025	0.04	0.24	1.02	1.12*	1.11
78	Q61176	Arg1	Arginase-1	0.25	0.038	0.52	0.61	-1.12	-1.1	-1.03
42	P16460	Ass1	Argininosuccinate synthase	0.15	0.011	0.62	0.8	-1.18	-1.22	-1.29
86	P16460	Ass1	Argininosuccinate synthase	0.3	0.049	0.65	0.55	-1.12	-1.16	-1.35
3	Q8C196	Cps1	Carbamoyl-phosphate synthase I	0.0049	0.00021	0.9	0.36	-1.31**	-1.15	-1.18
9	Q8C196	Cps1	Carbamoyl-phosphate synthase I	0.014	0.00081	0.52	0.37	-1.29**	-1.13	-1.14
11	P26443	Glud1	Glutamate dehydrogenase 1. mitochondrial precursor	0.026	0.0011	0.54	0.87	-1.13	-1.13	-1.18
Cholesterol and lipid metabolic processes										
12	Q920E5	Fdps	Farnesyl pyrophosphate synthetase	0.0032	0.0012	0.31	0.019	-1.05	1.37*	1.65**
66	Q920E5	Fdps	Farnesyl pyrophosphate synthetase	0.064	0.026	0.091	0.51	1.07	1.13	1.32
19	P52430	Pon1	Serum paraoxonase/arylesterase 1	0.048	0.0033	0.72	0.4	-1.15	-1.36*	-1.12
55	Q9QXE0	Hacl1	2-hydroxyphytanoyl-CoA lyase	0.097	0.015	0.38	0.41	1.05	1.15	1.07
45	P50544	Acadvl	Acyl-CoA dehydrogenase. very-long-chain specific. mitochondrial precursor	0.02	0.012	0.019	0.87	-1.08	-1.13	-1.11
81	Q8VCW8	Acsf2	Acyl-CoA synthetase family member 2. mitochondrial	0.043	0.042	0.19	0.1	-1.01	1.19	1.06*
26	Q8BWT1	Acaa2	3-ketoacyl-CoA thiolase. mitochondrial	0.041	0.0048	0.31	0.42	-1.1	-1.04	-1.13

68	Q8VCC1	Hpgd	5-hydroxyprostaglandin dehydrogenase [NAD+]	0.16	0.027	0.91	0.29	1.1	1.43	1.14
2	P06801	Me1	NADP-dependent malic enzyme	0.0029	0.00019	0.13	0.53	1.16	1.26**	1.14
37	Q91V92	Acly	ATP citrate lyase	0.036	0.0088	0.38	0.083	-1.01	1.22*	1.17
35	P56480	Atp5b	ATP synthase beta chain. mitochondrial precursor	0.033	0.0081	0.067	0.8	-1.09	-1.05	-1.1
Protein metabolic processes										
80	Q8BWY3	Etf1	Eukaryotic peptide chain release factor subunit 1	0.05	0.041	0.64	0.035	1.05	-1.42**	-1.1
43	P49722	Psma2	Proteasome subunit alpha type-2	0.12	0.011	0.67	0.48	1.04	1.13	1.12
64	O88685	Psmc3	26S protease regulatory subunit 6A	0.12	0.023	0.88	0.18	1.01	1.13	1.36*
77	P62334	Psmc6	26S protease regulatory subunit S10B	0.0032	0.038	6E-05	0.52	-1.03	-1.09	-1.03
46	P97371	Psme1	Proteasome activator complex subunit 1	0.15	0.013	0.58	0.77	1.07	1.11	1.14
75	Q9D0R2	Tars	Threonyl-tRNA synthetase. cytoplasmic	0.047	0.033	0.034	0.75	1.06	1.03	1.08
Other metabolic processes										
92	Q80X81	Acat3	acetyl-Coenzyme A acetyltransferase 3	0.03	0.12	0.29	0.015	-1.07	1.12	1.08
62	P97355	Srm	Spermidine synthase	0.11	0.021	0.28	0.36	1.25	1.06	1.34
14	Q99MR8	Mccc1	Methylcrotonoyl-CoA carboxylase alpha chain. mitochondrial precursor	0.0094	0.0014	0.0049	0.08	-1.15**	-1.09	-1.01
6	P40142	Tkt	Transketolase	0.00088	0.00044	0.0091	0.16	1.03	1.14**	1.13
23	P40142	Tkt	Transketolase	0.014	0.004	0.11	0.29	1.14	1.5*	1.25
22	Q99LB7	Sardh	Sarcosine dehydrogenase. mitochondrial precursor	0.026	0.0038	0.11	0.72	-1.07	-1.05	-1.1
54	Q9DBT9	ME2GLYDH	Dimethylglycine dehydrogenase. mitochondrial precursor	0.17	0.015	0.58	0.73	-1.14	-1.06	-1.09
27	Q8VC30	Dak	Bifunctional ATP-dependent dihydroxyacetone kinase/FAD-AMP lyase	0.023	0.0048	0.42	0.1	1	1.28*	1.26
70	Q8VC30	Dak	Bifunctional ATP-dependent dihydroxyacetone kinase/FAD-AMP lyase	0.077	0.028	0.22	0.24	1	1.14	1.08
63	Q9CWS0	Ddah1	NG.NG-dimethylarginine dimethylaminohydrolase 1	0.12	0.021	0.14	0.79	1.05	1.1	1.07

24	P52196	Tst	Thiosulfate sulfurtransferase	0.0097	0.0041	0.025	0.5	1.19	1.38	1.07
94	P00920	Ca2	Carbonic anhydrase 2	0.000071	0.32	5E-06	0.98	1.06	1.07	1.04
10	Q78JT3	Haao	3-hydroxyanthranilate 3.4-dioxygenase	0.012	0.001	0.46	0.22	1.03	1.13	1.14*
76	Q922D8	Mthfd1	C-1-tetrahydrofolate synthase. cytoplasmic	0.076	0.034	0.2	0.21	-1.02	1.21	1.29
Chaperone										
71	P38647	GRP 75	Stress-70 protein. mitochondrial precursor	0.0013	0.03	0.0003	0.58	-1.11	-1.03	-1.11
36	P63038	Hspd1	60 kDa heat shock protein. mitochondrial precursor	0.013	0.0085	0.014	0.78	-1.09	-1.11	-1.06
67	P63038	Hspd1	60 kDa heat shock protein. mitochondrial precursor	0.23	0.027	0.44	0.89	-1.16	-1.12	-1.09
57	Q8CGK3	Lonp1	Lon protease homolog	0.16	0.017	0.87	0.41	-1.08	-1.04	-1.16
79	Q8CGK3	Lonp1	Lon protease homolog	0.064	0.038	0.083	0.38	-1.01	-1.04	-1.08
60	P17742	Ppia	Peptidyl-prolyl cis-trans isomerase	0.08	0.021	0.23	0.33	1.04	1.19	1.07
95	P24369	Ppib	Peptidyl-prolyl cis-trans isomerase B	0.021	0.36	0.079	0.014	-1.03	-1.23	1.14
8	P09103	P4hb	Protein disulfide-isomerase	0.005	0.00081	0.059	0.38	1.17	1.1	1.27**
Secreted										
89	P07724	Alb	Serum albumin precursor	0.00019	0.061	5E-05	0.12	-1.1	1.03	-1.18
44	Q921I1	Tf	Serotransferrin precursor	0.01	0.011	0.012	0.45	-1.06	-1.26	-1.19
83	Q921I1	Tf	Serotransferrin precursor	0.036	0.043	0.35	0.033	1.13	-1.29	-1.4*
87	Q921I1	Tf	Serotransferrin precursor	0.15	0.049	0.94	0.12	1.05	-1.21	-1.31
90	P04938	Mup8 and 10	Major urinary proteins 11 and 8	0.043	0.076	0.082	0.19	-1.07	-1.7	-1.05
cytoskeleton										
29	P40124	Cap1	Adenylyl cyclase-associated protein 1	0.042	0.0054	0.27	0.43	-1.39	-1.3	-1.1
20	P68134	Acta1	Actin. alpha skeletal muscle	0.048	0.0033	0.72	0.4	-1.15	-1.36*	-1.12
Xenobiotic metabolism										
84	P24472	Gsta4	Glutathione S-transferase 5.7	0.13	0.044	0.19	0.48	-1.04	-1.1	-1.22
1	P15626	Gstm2	Glutathione S-transferase Mu 2	0.00004	5.10E-06	0.26	0.005	1.04	1.56	1.66**
52	O35660	Gstm6	Glutathione S-transferase Mu 6	0.11	0.015	0.78	0.25	1.03	1.17*	1.08

61	P19157	Gstp1	Glutathione S-transferase P 1	0.078	0.021	0.34	0.35	-1.04	-1.32	-1.24
28	Q9WVL0	Gstz1	Maleylacetoacetate isomerase	0.032	0.0052	0.14	0.54	1.05	1.12	1.08
21	P08228	Sod1	Superoxide dismutase [Cu-Zn]	0.042	0.0034	0.48	0.45	1.08	1.14	1.06
18	P09671	Sod2	Superoxide dismutase	0.033	0.0031	0.56	0.28	-1.02	-1.08**	-1.04
51	Q9QXF8	Gnmt	Glycine N-methyltransferase	0.047	0.014	0.22	0.35	1.02	1.16	1.14
96	Q9QXF8	Gnmt	Glycine N-methyltransferase	0.023	0.9	0.0045	0.33	-1.09	1.09	-1.03
74	P40936	Inmt	Indolethylamine N-methyltransferase	0.094	0.031	0.81	0.098	1.07	1.4**	1.01
16	O55060	Tpmt	Thiopurine S-methyltransferase	0.02	0.0018	0.68	0.19	1.09	1.05	1.2**
15	Q91VF2	Hnmt	Histamine N-methyltransferase	0.038	0.0015	0.7	0.82	1.16	1.22	1.25
91	P50247	Ahcy	Adenosylhomocysteinase	0.0044	0.092	0.0003	0.02	1.2	-1.12	1.18
34	Q60967	Papss1	Bifunctional 3'-phosphoadenosine 5'-phosphosulfate synthase 2	0.038	0.0075	0.23	0.27	1.07	1.27*	1.1
33	P26443	Glud1	Glutamate dehydrogenase 1. mitochondrial precursor	0.0043	0.0068	0.035	0.72	-1.07	-1.1	-1.11*
Apoptosis										
65	Q9Z0X1	Aifm1	Programmed cell death protein 8. mitochondrial precursor	0.074	0.024	0.012	0.51	-1.11	-1.03	-1.05
47	Q91VD9	Ndufs1	NADH-ubiquinone oxidoreductase 75 kDa subunit. mitochondrial	0.0063	0.013	0.012	0.13	-1.09	-1.01	-1.17*
53	P05784	Krt18	Keratin. type I cytoskeletal 18	0.063	0.015	0.23	0.31	1.03	1.18	1.27
Not listed										
40	Q00896	Serpina1c	Alpha-1-antitrypsin 1-3	0.11	0.0098	0.62	0.56	-1.1	-1.34	-1.29
31	Q00897	Serpina1d	Alpha-1-antitrypsin 1-4 precursor	0.004	0.0065	0.0033	0.79	-1.13	-1.2	-1.14
73	P00920	Ca2	Carbonic anhydrase 2	0.002	0.031	3E-05	0.62	1.1	1.21	1.07
5	Q01768	Nme2	Nucleoside diphosphate kinase B	0.0053	0.00028	0.2	0.69	1.11	1.08	1.13*
7	Q63836	Selenbp2	Selenium-binding protein 2	0.001	0.00079	0.29	0.004	-1.03	1.16**	1.16**
48	Q9QYG0	Ndrg2	Isoform 1 of Protein NDRG2	0.14	0.013	0.8	0.42	-1.09	1.06*	-1.3
13	Q8R086	Suox	Sulfite oxidase. mitochondrial precursor	0.00061	0.0013	0.0013	0.22	-1.09	-1.08	-1.22**

41	Q9CZ13	Uqcrc1	Ubiquinol-cytochrome-c reductase complex core protein I. mitochondrial precursor	0.15	0.01	1	0.57	1.08	-1.03	-1.06
38	P70296	Pebp1	Phosphatidylethanolamine-binding protein 1	0.079	0.0093	0.22	0.97	1.13	1.15	1.14

Table 1: Protein identification of differentially expressed proteins in from mouse liver after exposure to CsA after 4, 11 and 25 days. [1]P-value from one way ANOVA statistical test between the six groups with each four biological replicates. [2]P-value from two way ANOVA (treatment) statistical test between the six groups, which indicates the differences between the control and exposed groups. [3]P-value from two way ANOVA (time) statistical test between the six groups, which indicates the differences between the day 4, 11 and 25. [4]P-value from two way ANOVA (interaction) statistical test between the six groups, which indicates the interaction between time and treatment. [5]The difference in the standardized abundance of the proteins is expressed as the fold change between the control (C) and the treated groups (T). The fold change is calculated by taking the means of standardized volume values for the protein spot in the corresponding groups (C=control, CsA=cyclosporin A, 4=day 4, 11=day 11, 25=day25), values are calculated as T/C and displayed in the range of +1 to + ∞ for increases in expression and calculated as-C/T and displayed in the range of -∞ to -1 for decreased expression. **Indicates significant fold changes ($P \leq 0.05$) between the control and the treated group, calculated with a multiple comparison test. *Indicates significant fold changes ($P \leq 0.1$) between the control and the treated group, calculated with a multiple comparison test.

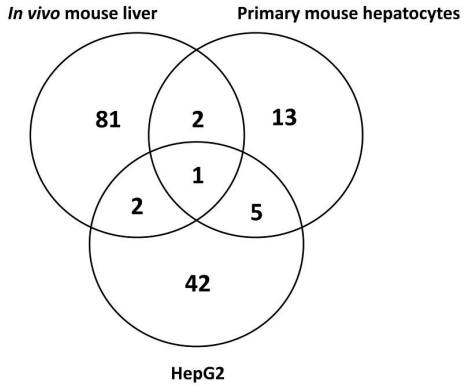

Figure 4: Venn diagram of the significant differentially expressed proteins induced by CsA in *in vivo* mouse liver, HepG2 and primary mouse hepatocytes.

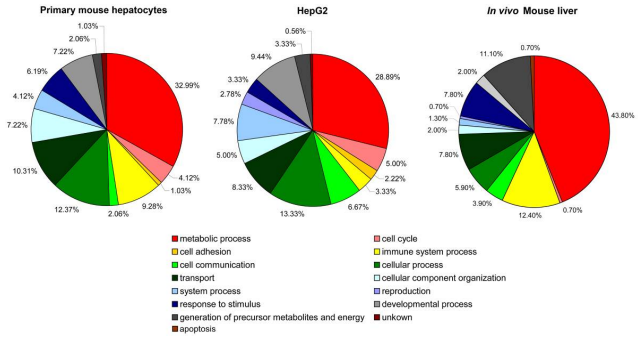

Figure 5: Classification of the differentially expressed proteins in primary mouse hepatocytes, HepG2 and liver after exposure to CsA with the Panther classification system (http://www.pantherdb.org).

Cluster	Function	Enrichment Score	*in vivo*	PMH	HepG2
1	ATP-binding	9.62041	40	5	16
2	Carbohydrate metabolism	9.293973	8	1	9
3	metal binding	7.999105	10	1	1
4	Methyltransferases	5.247008	4	1	0
5	metal binding	4.844126	8	2	5
6	NAD cofactor	4.807059	1	0	3
7	Detoxification glutathione S-transferase	4.368559	5	0	0
8	Chaperone activity	3.910156	1	7	9
9	Cytoskelet	3.231529	1	1	5
10	mRNA processing	2.748475	0	0	5
11	Protein transport	1.503542	1	1	1
12	response to organic substrate	0.489311	2	1	0

Table 2: Gene classification of the differentially expressed proteins after CsA treatment *in vivo*, primary mouse hepatocytes and HepG2.

Discussion

The aim of this study was to identify cholestatic-specific mechanisms *in vivo*, with use of proteomics. In addition, an *in vitro-in vivo* comparison of CsA-induced protein expression profiles was established by comparing these results with the results from our previous *in vitro* studies with HepG2 and primary mouse hepatocytes [9,10] For this purpose, we analyzed the hepatic protein expression in C57BL/6 mice after CsA-induced cholestasis. The cholestatic phenotype was established after 25 days and confirmed by histopathology and serum parameters, which allowed us to search for cholestatic-specific mechanisms *in vivo*.

Differential protein expression in mice after CsA treatment

CsA inhibits the bile salt export pump (ABCB11), multidrug resistance protein 2 (ABCC2) and P-glycoprotein (ABCB1) in the canalicular membrane vesicles. These ATP Binding Cassette transporters (ABC transporters) are responsible for the bile secretion into the bile canaliculus [14]. Therefore, inhibition of these transport proteins causes the hepatic accumulation of bile salts resulting in cholestasis [15]. Previous studies suggest that accumulated bile acids induce oxidative stress and can cause mitochondrial dysfunction in the liver [16]. Moreover, CsA induced *in vitro* as well as *in vivo* oxidative stress, increases lipid peroxidation and depletes the hepatic pool of glutathione [17,18] Superoxide is one of the main reactive oxygen species in the cell which can be converted into oxygen and hydrogen peroxide by superoxide dismutase. In our study cytoplasmatic superoxide dismutase 1 was up-regulated after cyclopsorin A treatment, while mitochondrial superoxide dismutase 2 was down-regulated, indicating that CsA induced oxidative stress and mitochondrial dysfunction. Indications for mitochondrial dysfunction are already visible after 4 days of CsA treatment, since all proteins with a significantly differential expression are mitochondrial.

Furthermore, the down-regulation of several enzymes contributing the TCA-cycle like aconitate hydratase, succinyl-CoA ligase (ADP-forming) subunit beta and methylmalonyl-coenzyme A mutase suggest a deficient ATP production by the mitochondria. Previously, others have demonstrated an ATP reduction in hepatocytes after exposure to necrotic concentrations of toxic bile salts [19,20]. The reduced ATP was directly due to mitochondrial dysfunction as glycolytic ATP generation was intact [20]. In our study several proteins from the glycolysis pathway were found to be up-regulated. This suggests a compensative mechanism for mitochondrial dysfunction via the glycolytic pathway.

Glutamate dehydrogenase is responsible for the conversion of glutamate to α-ketoglutarate and ammonium, which will bled off to the urea-cycle. The first step of the urea cycle requires ATP for the conversion of NH_4^+ and HCO_3^- to carbamoyl phosphate, catalyzed by carbamoyl-phosphate synthase (Cps1). In a later step, ATP is necessary for the conversion of citrulline and aspartate in argininosuccinate, catalyzed by argininosuccinate synthase (Ass1). In our study glutamate dehydrogenase 1, Ass1 and Cps1, were all down-regulated together with other enzymes from the urea cycle.

Rare autosomal recessive disorders of the urea cycle like arginase deficiency and citrin deficiency are associated with neonatal intrahepatic cholestasis [21,22]. Neonatal intrahepatic cholestasis is defined as impaired bilirubin excretion, resulting in jaundice and conjugated hyperbilirubinemia, detected either in a newborn or an infant up to 4 months old [21-23]. The pathogenesis of cholestasis in these urea cycle disorders remains unclear, probably the combination of a primary mitochondrial defect and a delayed maturity of bile acid metabolism, may form a vicious circle in transient neonatal intrahepatic cholestasis [22]. A similar mechanism for cholestasis as observed in neonatal intrahepatic cholestasis may explain down-regulation of enzymes from the urea cycle in our study.

Methylation enzymes indolethylamine N-methyltransferase (Inmt), thiopurine S-methyltransferase, glycine N-methyltransferase and histamine N-methyltransferase showed an increased expression after CsA treatment. Methyl conjugation is mainly used for the metabolism of small endogenous compounds such as epinephrine, norepinephrine, dopamine, and histamine but is also involved in the metabolism of macromolecules such as nucleic acids and in the biotransformation of certain drugs [24]. In contrast to other conjugative reactions, methylation leads to less polar compounds that may be less readily excreted from the body [24]. Inmt, thiopurine S-methyltransferase, glycine N-methyltransferase and histamine N-methyltransferase all use S-adenosylmethionine as methyldonor. Previously, it was shown that S-adenosylmethionine protects against CsA [25-26], chlorpromazine [27] and ethenylestradiol-induced cholestasis [28]. Cholestatic rat liver, induced by common bile duct ligation, exhibited increased enzymatic activities of Inmt and thiol methyltransferase [29].

The increased expression of these N-methyltransferases results in an increased conversion of S-adenosylmethionine to S-adenosyl-homocysteine, which in turn is converted in homocysteine and adenosine by adenosylhomocysteinase, here differentially expressed. The increased conversion of S-adenosylmethionine and S-adenosyl-homocystein activates the trans-sulfuration pathway, leading to the formation of glutathione [27]. Glutathione is responsible for the detoxification of various compounds to protect the cells from oxidative stress. Moreover it plays an important role in bile formation [30]. Previously it has been demonstrated that glutathione is depleted during cholestasis, therefore activation of the trans-sulfuration pathway is necessary to maintain the glutathione levels in the cholestasic liver [30,31]. In addition, sulfite oxidase and bifunctional 3'-phosphoadenosine 5'-phosphosulfate synthase 2, other enzymes of the trans-sulfuration pathway, were also differentially expressed.

Glutathione is a substrate of both conjugation and reduction reactions, catalyzed by glutathione S-transferase enzymes. Mice exposed to CsA, show a differential expression of several glutathione S-transferases (GSTs). GSTs are not only important phase II detoxification enzymes; they are able to bind bile acids and are thought to play a role in the intracellular trafficking of bile acids [32].

Furthermore, CsA induced the differential expression of proteins related to cholesterol biosynthesis and lipid metabolism. Bile acid synthesis is the main route for cholesterol metabolism and is initiated by cholesterol 7α-hydroxylase (CYP7A1). In our study Farnesyl diphosphate synthase (Fdps) showed an increased expression after 11 days of CsA exposure. Fdps is responsible for the formation of farnesyldiphosphate, a key intermediate in cholesterol synthesis and protein farnesylation. Previously drug-induced cholestasis was associated with an increased hepatic cholesterol synthesis, which is in line with the presently observed Fdps expression [33].

In addition, cholesterol synthesis requires the presence of cytosolic acetyl-coA. Previously, we mentioned a down-regulation of the TCA-cycle, a mitochondrial source of acetyl-coA. The up-regulation of citrate-lyase and NADP-dependent malic enzyme in our study, suggests a drain of mitochondrial acetyl-coA to the cytosol for cholesterol synthesis.

Furthermore, an increased cholesterol synthesis is associated with a decreased CYP7A1 expression as a protective adaptive response to reduce cellular bile accumulation [33]. Probably these two mechanisms are the cause of high plasma cholesterol in cholestasis. In a previous study, in which transcriptomics analysis was performed on liver samples used for proteome analysis in this study, CYP7A1 down-regulation was observed as one of the strongest effects upon progression of cholestasis in mice and was interpreted as an adaptive response [34].

Serum paraoxonase/arylesterase 1 (Pon1) is an antioxidant enzyme responsible for the detoxification of organophosphates and prevention

of low-density lipoprotein oxidative modification. Our study shows a down-regulation of Pon1 after CsA treatment. Rats treated with CCl_4 showed a reduced activity of hepatic Pon1 together with increased lipid peroxidation [35]. Furthermore, Pon1 was down-regulated in the protein extract from rat liver exposed to acetaminophen [36] However, Pon1 failed as candidate marker for drug-induced hepatotoxicity, because it was not consistently altered in response to several hepatotoxicants [37].

In vivo-in vitro comparison

Previously we analyzed CsA-induced cholestasis in HepG2 cells [9] and in primary mouse hepatocytes [10]. An *in vivo-in vitro* comparison of CsA-induced hepatotoxicity based on single protein expression is difficult, partly because there is only a small overlap in the differentially expressed proteins from the different models (Figure 4). Therefore the differentially expressed proteins from these models were classified based on the GO-terms with the Panther classification system. This classification revealed a similar outcome for HepG2 and primary mouse hepatocytes. The majority of the differentially expressed proteins are involved in metabolic processes, cellular processes and transport. Similar processes between the analyzed *in vitro* systems are cell cycle, cellular processes, developmental processes and cell adhesion (Figure 5). In all three models CsA altered proteins belonging to transport and a response to stimulus (Figure 5). For a more detailed overview the proteins were clustered according to their function with DAVID Bioinformatics Resources 6.7. Cluster 1, 2 and 5 contain differentially expressed proteins from the three models. Cluster 1 involves ATP-binding and mitochondrial proteins and cluster 2 contains proteins from carbohydrate metabolism. Cluster 5 refers to binding of metal ions, which is a characteristic of many metabolic enzymes like the glycolytic enzymes. These clusters show that CsA induces *in vivo* as well as *in vitro* mitochondrial dysfunction and changes in the energy metabolism, as also described before. Mitochondria are critical targets for drug toxicity; therefore mitochondrial dysfunction and oxidative stress are often seen in drug-induced hepatotoxicity [38]. The differential expressions of proteins from energy metabolism are probably a first indication of a toxicological response. However, several proteins from energy metabolism are often detected in comparative proteomics and considered as proteins from a general stress response [39]. Therefore using those proteins as specific markers for cholestasis should be done with caution.

Methyltransferases which are described earlier as detoxifying enzymes constitute cluster 4. Almost all methyltransferases were detected only *in vivo*, however Inmt was also detected in primary mouse hepatocytes. Furthermore, *in vivo* CsA induced cholestasis was accompanied with the differential expression of glutathione-S-transferases (cluster 7). In primary mouse hepatocytes we have also detected some glutathione-S-transferases, although they were not significantly changed after CsA treatment and were therefore excluded from the cluster analysis. We believe that both methyltransferases and glutathione-S-transfereses are important detoxification proteins in CsA-induced cholestasis. These proteins were mainly detected *in vivo* but some also in primary mouse hepatocytes. However, they were not observed in HepG2, suggesting an under-representation of drug-metabolizing enzymes in HepG2 [40,41].

Characteristic for HepG2 cells, proteins responsible for mRNA processing were differentially expressed (cluster 10). These proteins have central roles in DNA repair, telomere elongation, cell signaling and in regulating gene expression at transcriptional and translational level [42]. Furthermore, heterogeneous nuclear ribonucleoproteins (hnRNPs) play a role in tumor development and are up-regulated in various cancers [42]. Previously it was shown that carcinoma cell lines including HepG2 cells have a higher expression of hnRNPs than human intestinal epithelium [43]. Therefore the expression of these proteins can be ascribed to the carcinoma character of the HepG2 cell line. Apparently CsA induced a down-regulation of these proteins and probably decreased cell proliferation.

In vitro, CsA mainly induced the differential expression of chaperone proteins (cluster 8), while this was less observed *in vivo*. Previously we hypothesized that CsA induces ER stress, with an altered chaperone activity together with a disturbed protein transport resulting in a decreased protein secretion [9]. However, this reaction of CsA seems characteristic for *in vitro* models. Possibly *in vitro* cell cultures are more sensitive because they are in direct contact with the toxicant and they function independent from other cells/organs.

Our analysis identified the similarities and differences in *in vitro* and *in vivo* models with respect to the response to CsA induced hepatotoxicity. Previous studies have shown the potential of the current *in vitro* models to detect drug-induced hepatotoxicity [2,9,44]. However the different toxicant-induced responses between *in vivo* and *in vitro* models explain the current difficulties to validate *in vitro* biomarkers against *in vivo* models.

Acknowledgments

This work was supported by the Netherlands Genomics Initiative/ Netherlands Organization for Scientific Research (NWO), [grant number: 050-060-510]. We thank Erik Royackers from the Biomedical Research Institute of Hasselt University for his technical support of the LC-MS/MS analysis. The authors thank Piet Beekhof and Dr. Eugene Janssen for clinical chemistry analyses and Joke Robinson for histopathology analyses.

References

1. Kienhuis AS, Wortelboer HM, Maas WJ, van Herwijnen M, Kleinjans JC, et al. (2007) A sandwich-cultured rat hepatocyte system with increased metabolic competence evaluated by gene expression profiling. Toxicol In Vitro 21: 892-901.
2. Mathijs K, Kienhuis AS, Brauers KJ, Jennen DG, Lahoz A, et al. (2009) Assessing the metabolic competence of sandwich-cultured mouse primary hepatocytes. Drug Metab Dispos 37: 1305-1311.
3. Jennen DG, Magkoufopoulou C, Ketelslegers HB, van Herwijnen MH, Kleinjans JC, et al. (2010) Comparison of HepG2 and HepaRG by whole-genome gene expression analysis for the purpose of chemical hazard identification. Toxicol Sci 115: 66-79.
4. Kienhuis AS, van de Poll MC, Wortelboer H, van Herwijnen M, Gottschalk R, et al. (2009) Parallelogram approach using rat-human in vitro and rat in vivo toxicogenomics predicts acetaminophen-induced hepatotoxicity in humans. Toxicol Sci 107: 544-552.
5. Heijne WH, Jonker D, Stierum RH, van Ommen B, Groten JP (2005) Toxicogenomic analysis of gene expression changes in rat liver after a 28-day oral benzene exposure. Mutat Res 575: 85-101.
6. de Longueville F, Atienzar FA, Marcq L, Dufrane S, Evrard S, et al. (2003) Use of a low-density microarray for studying gene expression patterns induced by hepatotoxicants on primary cultures of rat hepatocytes. Toxicol Sci 75: 378-392.
7. Greenbaum D, Colangelo C, Williams K, Gerstein M (2003) Comparing protein abundance and mRNA expression levels on a genomic scale. Genome Biol 4: 117.

8. Minden J (2007) Comparative proteomics and difference gel electrophoresis. Biotechniques 43: 739, 741, 743 passim.
9. Van Summeren A, Renes J, Bouwman FG, Noben JP, van Delft JH, et al. (2011) Proteomics investigations of drug-induced hepatotoxicity in HepG2 cells. Toxicol Sci 120: 109-122.
10. Van Summeren A, Renes J, Lizarraga D, Bouwman FG, Noben JP, et al. (2013) Screening for drug-induced hepatotoxicity in primary mouse hepatocytes using acetaminophen, amiodarone, and cyclosporin a as model compounds: an omics-guided approach. OMICS 17: 71-83.
11. Rotolo FS, Branum GD, Bowers BA, Meyers WC (1986) Effect of cyclosporine on bile secretion in rats. Am J Surg 151: 35-40.
12. Bouwman FG, Claessens M, van Baak MA, Noben JP, Wang P, et al. (2009) The Physiologic Effects of Caloric Restriction Are Reflected in the in Vivo Adipocyte-Enriched Proteome of Overweight/Obese Subjects. J Proteome Res 8: 5532-5540.
13. Dumont D, Noben JP, Raus J, Stinissen P, Robben J (2004) Proteomic analysis of cerebrospinal fluid from multiple sclerosis patients. Proteomics 4: 2117-2124.
14. Trauner M, Boyer JL (2003) Bile salt transporters: molecular characterization, function, and regulation. Physiol Rev 83: 633-671.
15. Alrefai WA, Gill RK (2007) Bile acid transporters: structure, function, regulation and pathophysiological implications. Pharm Res 24: 1803-1823.
16. Kaplan MM (1994) Primary biliary cirrhosis--a first step in prolonging survival. N Engl J Med 330: 1386-1387.
17. Wolf A, Trendelenburg CF, Diez-Fernandez C, Prieto P, Houy S, et al. (1997) Cyclosporine A-induced oxidative stress in rat hepatocytes. J Pharmacol Exp Ther 280: 1328-1334.
18. Jimenez R, Galan AI, Gonzalez de Buitrago JM, Palomero J, Munoz ME (2000) Glutathione metabolism in cyclosporine A-treated rats: dose- and time-related changes in liver and kidney. Clin Exp Pharmacol Physiol 27: 991-996.
19. Spivey JR, Bronk SF, Gores GJ (1993) Glycochenodeoxycholate-induced lethal hepatocellular injury in rat hepatocytes. Role of ATP depletion and cytosolic free calcium. J Clin Invest 92: 17-24.
20. Gores GJ, Miyoshi H, Botla R, Aguilar HI, Bronk SF (1998) Induction of the mitochondrial permeability transition as a mechanism of liver injury during cholestasis: a potential role for mitochondrial proteases. Biochim Biophys Acta 1366: 167-75.
21. Gomes Martins E, Santos Silva E, Vilarinho S, Saudubray JM, Vilarinho L (2010) Neonatal cholestasis: an uncommon presentation of hyperargininemia. J Inherit Metab Dis 33 Suppl 3: S503-506.
22. Tazawa Y, Abukawa D, Sakamoto O, Nagata I, Murakami J, et al. (2005) A possible mechanism of neonatal intrahepatic cholestasis caused by citrin deficiency. Hepatol Res 31: 168-71.
23. Moyer V, Freese DK, Whitington PF, Olson AD, Brewer F, et al. (2004) Guideline for the evaluation of cholestatic jaundice in infants: recommendations of the North American Society for Pediatric Gastroenterology, Hepatology and Nutrition. J Pediatr Gastroenterol Nutr 39: 115-128.
24. Lohr JW, Willsky GR, Acara MA (1998) Renal drug metabolism. Pharmacol Rev 50: 107-141.
25. Galan AI, Munoz ME, Jimenez R (1999) S-Adenosylmethionine protects against cyclosporin A-induced alterations in rat liver plasma membrane fluidity and functions. J Pharmacol Exp Ther 290: 774-781.
26. Fernández E, Galán AI, Morán D, González-Buitrago JM, Muñoz ME, et al. (1995) Reversal of cyclosporine A-induced alterations in biliary secretion by S-adenosyl-L-methionine in rats. J Pharmacol Exp Ther 275: 442-449.
27. Friedel HA, Goa KL, Benfield P (1989) S-adenosyl-L-methionine. A review of its pharmacological properties and therapeutic potential in liver dysfunction and affective disorders in relation to its physiological role in cell metabolism. Drugs 38: 389-416.
28. Boelsterli UA, Rakhit G, Balazs T (1983) Modulation by S-adenosyl-L-methionine of hepatic Na+,K+-ATPase, membrane fluidity, and bile flow in rats with ethinyl estradiol-induced cholestasis. Hepatology 3: 12-17.
29. Kim YH, Joo 2nd (2001) Arylamine N-methyltransferase and thiol methyltransferase activities in cholestatic rat liver induced by common bile duct ligation. Exp Mol Med 33: 23-28.
30. Tiao MM, Lin TK, Wang PW, Chen JB, Liou CW (2009) The role of mitochondria in cholestatic liver injury. Chang Gung Med J 32: 346-353.
31. Vendemiale G, Grattagliano I, Lupo L, Memeo V, Altomare E (2002) Hepatic oxidative alterations in patients with extra-hepatic cholestasis. Effect of surgical drainage. J Hepatol 37: 601-605.
32. Agellon LB, Torchia EC (2000) Intracellular transport of bile acids. Biochim Biophys Acta 1486: 198-209.
33. Chisholm JW, Nation P, Dolphin PJ, Agellon LB (1999) High plasma cholesterol in drug-induced cholestasis is associated with enhanced hepatic cholesterol synthesis. Am J Physiol 276: G1165-73.
34. Kienhuis AS, Vitins AP, Pennings JL, Pronk TE, Speksnijder EN, et al. (2013) Cyclosporine A treated in vitro models induce cholestasis response through comparison of phenotype-directed gene expression analysis of in vivo Cyclosporine A-induced cholestasis. Toxicol Lett 221: 225-236.
35. Ferre N, Camps J, Cabre M, Paul A, Joven J (2001) Hepatic paraoxonase activity alterations and free radical production in rats with experimental cirrhosis. Metabolism 50: 997-1000.
36. Amacher DE, Adler R, Herath A, Townsend RR (2005) Use of proteomic methods to identify serum biomarkers associated with rat liver toxicity or hypertrophy. Clin Chem 51: 1796-1803.
37. Adler M, Hoffmann D, Ellinger-Ziegelbauer H, Hewitt P, Matheis K, et al. (2010) Assessment of candidate biomarkers of drug-induced hepatobiliary injury in preclinical toxicity studies. Toxicol Lett 196: 1-11.
38. Jaeschke H, McGill MR, Ramachandran A (2012) Oxidant stress, mitochondria, and cell death mechanisms in drug-induced liver injury: lessons learned from acetaminophen hepatotoxicity. Drug Metab Rev 44: 88-106.
39. Wang P, Bouwman FG, Mariman EC (2009) Generally detected proteins in comparative proteomics--a matter of cellular stress response? Proteomics 9: 2955-2966.
40. Boess F, Kamber M, Romer S, Gasser R, Muller D, et al. (2003) Gene expression in two hepatic cell lines, cultured primary hepatocytes, and liver slices compared to the in vivo liver gene expression in rats: possible implications for toxicogenomics use of in vitro systems. Toxicol Sci 73: 386-402.
41. Wilkening S, Bader A (2003) Influence of culture time on the expression of drug-metabolizing enzymes in primary human hepatocytes and hepatoma cell line HepG2. J Biochem Mol Toxicol 17: 207-213.
42. Carpenter B, MacKay C, Alnabulsi A, MacKay M, Telfer C, et al. (2006) The roles of heterogeneous nuclear ribonucleoproteins in tumour development and progression. Biochim Biophys Acta 1765: 85-100.
43. Lenaerts K, Bouwman FG, Lamers WH, Renes J, Mariman EC (2007) Comparative proteomic analysis of cell lines and scrapings of the human intestinal epithelium. BMC Genomics 8: 91.
44. Wang K, Shindoh H, Inoue T, Horii I (2002) Advantages of in vitro cytotoxicity testing by using primary rat hepatocytes in comparison with established cell lines. J Toxicol Sci 27: 229-37.